Revista de Metalurgia
October-December 2023, 59 (4), e253
ISSN-L: 0034-8570
https://doi.org/10.3989/revmetalm.253

Investigations on microstructure, hardness and tribological behaviour of AA7075-Al_2O_3 composites synthesized via stir casting route

Mathusoothana Perumal Ezhilan[a], Loganathan Emmanual[b], Sivasamy Alagarsamy[c,*], Meiyanathan Meignanamoorthy[d]

[a] Department of Mechanical Engineering, Rohini College of Engineering and Technology, Kanyakumari-629 401, Tamil Nadu, India

[b] Department of Mechanical Engineering, M. Kumarasamy College of Engineering, Karur-639 113, Tamil Nadu, India

[c] Department of Mechanical Engineering, Mahath Amma Institute of Engineering and Technology, Pudukkottai-622 101, Tamil Nadu, India

[d] Department of Mechanical Engineering, Chendhuran College of Engineering and Technology, Pudukkottai-622 507, Tamil Nadu, India

(*Corresponding author: s.alagarsamy88@gmail.com)

Submitted: 9 September 2022; Accepted: 1 December 2023; Available On-line: 3 January 2024

ABSTRACT: Aluminium matrix composite (AMC) materials play an important role in the field of automobile and aerospace industries due to their excellent properties. In this research, aluminium alloy (AA7075) was reinforced with alumina (Al_2O_3) particles to improve their hardness and tribological behaviour of the base alloy. Four composites were prepared by varying the content (4, 8 and 12 wt.%) of Al_2O_3 particles through the stir casting technique. The surface morphology of the proposed composites ensured the uniform distribution of Al_2O_3 particles into the matrix alloy. The hardness of the composite was measured using a Brinell hardness tester and the maximum value of hardness was found in the AA7075 – 8 wt.% Al_2O_3 composite. Hence, a tribological investigation was carried out on this AA7075 – 8 wt.% Al_2O_3 composite. Load (P), sliding speed (V) and sliding velocity (D) were taken as the wear parameters for conducting the experiments. A Technique for Order Preference by Similarity to Ideal Preferred Solution (TOPSIS) approach has been applied to find out the optimal conditions of parameters to obtain the lowest wear rate (WR) and the co-efficient of friction (COF). The results showed that the lowest WR and COF was obtained at ‘P’ of 15 N, ‘V’ of 1 $m \cdot s^{-1}$ and ‘D’ of 1000 $m \cdot s^{-1}$. ANOVA results revealed that ‘P’ is the factor with the most significant contribution (38.36%), followed by ‘D’ (28.32%). The worn surface morphology of the confirmation experiment specimen was investigated by SEM and the wear mechanism was reported.

KEYWORDS: AA7075; Al_2O_3;; Composites; Hardness; Stir casting; TOPSIS approach; Tribological behaviour

Citation/Citar como: Ezhilan, M.; Emmanual, L.; Alagarsamy, S.V.; Meignanamoorthy, M. (2023). “Investigations on microstructure, hardness and tribological behaviour of AA7075-Al_2O_3 composites synthesized via stir casting route”. *Rev. Metal.* 59(4): e253. https://doi.org/10.3989/revmetalm.253

RESUMEN: *Investigación de la microestructura, dureza y comportamiento tribológico de los materiales compuestos AA7075-Al_2O_3 sintetizados mediante moldeo por agitación.* Los materiales compuestos de matriz de aluminio (MCMA) juegan un papel importante en el campo de la automoción y la industria aeroespacial debido a sus excelentes propiedades. En esta investigación, se reforzó la aleación de aluminio AA7075 con partículas de alúmina (Al_2O_3) para mejorar su dureza y el comportamiento tribológico de la aleación base. Se prepararon cuatro materiales compuestos variando el contenido (4, 8 y 12 % en peso) de partículas de Al_2O_3 mediante la técnica de moldeo por agitación. La morfología superficial de los compuestos propuestos garantizaba la distribución uniforme de las partículas de Al_2O_3 en la aleación matriz. La dureza del material compuesto se midió utilizando un durómetro Brinell y el valor máximo de dureza se encontró en el material compuesto AA7075 - 8 % Al_2O_3. Por lo tanto, se llevó a cabo una investigación tribológica en este compuesto AA7075 - 8 % Al_2O_3. La carga (P), la velocidad de deslizamiento (V) y la velocidad de deslizamiento (D) se tomaron como parámetros de desgaste para llevar a cabo los experimentos. Se aplicó una técnica de orden de preferencia por similitud a la solución ideal preferida (TOPSIS) para determinar las condiciones óptimas de los parámetros que permitieran obtener la tasa de desgaste (WR) y el coeficiente de fricción (COF) más bajos. Los resultados mostraron que el menor WR y COF se obtuvieron con 'P' de 15 N, 'V' de 1 $m \cdot s^{-1}$ y 'D' de 1000 $m \cdot s^{-1}$. Los resultados del ANOVA revelaron que "P" es el factor con la contribución más significativa (38,36%), seguido de "D" (28,32%). La morfología de la superficie desgastada de la probeta del experimento de confirmación se investigó mediante SEM y se informó del mecanismo de desgaste.

PALABRAS CLAVE: AA7075; Al_2O_3; Composites; Comportamiento tribológico; Dureza; Enfoque TOPSIS; Fundición por agitación

ORCID ID: I. M. Ezhilan (https://orcid.org/0000-0002-1970-9795); L. Emmanual (https://orcid.org/0000-0002-4027-3922); S.V. Alagarsamy (https://orcid.org/0000-0002-6564-0346); M. Meignanamoorthy (https://orcid.org/0000-0001-8823-4343).

1. INTRODUCTION

Aluminium metal matrix composites (AMMCs) are widely preferred engineering material rather than unreinforced alloys in the development of new products in order to improve the overall performance of the product. AMMCs are utilized in aerospace, marine, automotive and defence industries due to its superior properties such as high strength with light weight, high hardness, high stiffness and more corrosion and wear resistance (Sambathkumar *et al.,* 2021). The properties can be tailored by combining the two or more elements in which the major element is called as matrix material whereas the minor element is called as the reinforcement. The reinforcements are added in the form of particles, whiskers or fibers which alters the properties of the matrix material (Alagarsamy and Ravichandran, 2019a; Johny James *et al.,* 2023). Generally, ceramics like oxides, carbides and nitrides are preferred as reinforcements in AMMCs for their low coefficient of thermal expansion with higher strength and hardness (Miyajima and Iwai, 2003). The properties of the AMMCs generally depend on the processing techniques like stir casting, infiltration, powder metallurgy, etc,. Therefore, it is more important to manufacture a product economically and also with a homogeneous distribution of reinforcing particles to make the AMMCs isotropic. Stir casting is one of the promising techniques to achieve a homogeneous distribution of the particles and also found to be economical compared to the other fabrication techniques (Sakthivelu *et al.,* 2018; Singh and Chauhan, 2019). The limitations of the stir casting process are slag formation and porosity due to high temperature involved. However, this method can be employed extensively due to its flexibility and favorable range of economics. Bharath *et al.* (2014) studied the properties of 6061 Al matrix composites filled with Al_2O_3 particles fabricated by liquid metallurgy route and they observed that the hardness, tensile strength and wear resistance were drastically improved with the increase in the Al_2O_3 content. Altinkok (2013) reported that an increasing trend in the addition of Al_2O_3/SiC particles increased the wear resistance of AMMCs. Huda *et al.* (2019) examined the mechanical and wear properties of Al_2O_3 reinforced AA7075 composites developed through stir casting. They understood that adding Al_2O_3 particles significantly improved the hardness and decreased WR. Bhowmik *et al.* (2021) developed the Al7075/TiB_2/SiC hybrid composites and they reported that the hardness and tensile strength of the composites drastically improved due to the addition of the reinforcing particles. Suresh *et al.* (2019) studied the mechanical properties of AA7075/Al_2O_3/SiC nano-metal matrix composites and they reported that the mechanical properties improved compared to those of the base alloy and also a homogeneous distribution was achieved by utilizing appropriate stir casting parameters. Akinwamide *et al.* (2019) synthesized aluminium reinforced with ferrotitanium and SiC composites and observed that the addition of SiC improved the hardness and that the formation of the oxide layer reduces the WR of the composites. Mistry and Gohil (2019) developed AMMCs reinforced with varying amounts of Si_3N_4 content. They reported that the addition of Si_3N_4 improves the mechanical properties and the wear loss of 12 wt.% Si_3N_4 AMMC was considerably reduced compared to the heat treated AA7075 base alloy. Jayakumar *et al.* (2018) studied the erosion behavior and hardness of AMCs reinforced with SiC particles synthesized through stir casting and centrifugal casting. They reported that the addition of SiC particles consistently improves the hardness and reduces the wear loss due to the inclusion of SiC particles. Alagarsamy *et al.* (2020) investigated the effect of wear parameters namely load, sliding velocity and sliding distance for the TiO_2 incorporated Al7075 alloy composites and concluded that the load has the primary decisive factor on reducing the WR and COF. Baskaran *et al.* (2014) studied the dry sliding wear behavior of AA7075-TiC composites using Taguchi technique and reported that the load and the sliding velocity were the more dominant factors on the WR. From the lot of earlier studies, we had understood that predicting the hardness and tribological behaviour of AMCs is a crucial process since it depends on more factors, such as 'P', 'V', and 'D'. Therefore, a complete statistical assessment is very important to find the wear behaviour of AMCs. Hence, the present study was made to investigate the effect of Al_2O_3 content on the hardness for the AA7075 matrix composites synthesized via stir casting route and also to find out the optimal conditions of wear parameters to obtain the lowest WR and COF for the proposed composites using TOPSIS approach.

2. MATERIALS AND METHODS

2.1. Experimental details

In this work, Aluminium 7xxx alloy (AA7075) was selected as the matrix material and alumina (Al_2O_3) was used as the reinforcement with an average particle size of 30 µm received from microtroniks lab chemicals. Among the aluminium alloy series, AA7075 has more significance in the automotive and aerospace industries for the development of gears and shafts, bicycle frame, aircraft fittings, missile parts and defense applications due to its strength to weight ratio, high toughness and natural aging characteristics (Moustafa *et al.,* 2022; Uros Stamenkovic *et al.,* 2023). The chemical composition (wt.%) of AA7075 is Zn-5.4, Mg-2.42, Cu-1.42, Fe-0.42, Cr-0.21, Si-0.13, Mn-0.12, Ti-0.11 and Al- to balance. Four composite specimens were prepared by varying the wt.% of Al_2O_3 particles viz plain AA7075, AA7075-4 wt.% Al_2O_3, AA7075-8 wt.% Al_2O_3 and AA7075-12 wt.% Al_2O_3. The composite samples were produced through bottom pouring type stir casting method. At first, pure AA7075 ingot was melted in graphite crucible using an electric furnace at the temperature of 800 °C and it was brought to 650 °C. Similarly, Al_2O_3 particles were preheated at 250 °C to remove the moisture and also to improve the wettability of the Al_2O_3 particles with molten AA7075. The molten AA7075 was stirred with a motorized agitator at a speed of 200 rpm constantly. Subsequently, the preheated Al_2O_3 particles were added slowly in the vortex of the AA7075 pool. Then, the mixture was constantly stirred at 250 rpm for 20 mins to achieve a homogeneous distribution of particles in the AA7075 pool. After stirring, the slurry was poured into the preheated steel die immediately. Figure 1 shows the experimental plan of the present study.

The surface morphology of the proposed composites were taken by using scanning electron microscopy (Vega3, Tescan model). The Brinell hardness test was carried out using ASTM E18 standard as a reference to measure the hardness of the different fabricated composite specimens. To perform the tribological behaviour studies, the composite sample was selected based on the hardness value obtained. Often, high hardness material possess good wear resistance. Hence, the higher hardness of the composite specimen was taken fo to study the tribological properties such as the WR and the COF respectively. A pin on disc tribometer was used to conduct the wear test under dry sliding conditions. The test pins were prepared using ASTM G-99 standard as a guide with a dimension of 10 mm in diameter and 32 mm in length by wire-cut electric discharge machining. In general, three factors namely load (P), sliding distance (D) and sling velocity (V) are control the WR and COF (Allasi *et al.,* 2023). Hece, these factors are taken as the input parameters and are provided in Table 1. Based on the parameters selection, the experiments were executed using a L_9 (3^3) orthogonal array (OA) as it is shown in Table 1. After the test, the WR and COF are measured by using Eq. (1) and (2) (Alagarsamy and Ravichandran, 2019b).

$$\text{Wear rate}\,(\text{mm}^3/\text{m}) = \frac{\Delta m / \rho}{D} \qquad (1)$$

$$\text{Coefficient of friction}, \mu = F_T / F_N \qquad (2)$$

where, Δm- mass loss of test specimen (grams), ρ – density of the composite (g·mm^{-3}), D- sliding distance (m), F_T- tangential force (N) and F_N- normal force (N).

2.2. Optimization using TOPSIS method

This method was proposed by Hwang and Yoon in 1981 to solve multi criteria decision making (MCDM) problems (Magibalan *et al.,* 2020). MCDM methods are used to solve the multi objective problems by the researchers to find out the optimum parameters from definite number of alternatives (Senthamarai *et al.,* 2023). Hence, in this study, TOPSIS approach was implemented to optimize the wear control parameters on estimated WR and COF. In the TOPSIS method, best solution is selected which should have the shortest distance to the positive ideal solution and the farthest to the negative ideal solution (Azadeh *et al.,* 2011). To determine the optimum levels of parameters, the given steps to be implemented and are as follows,

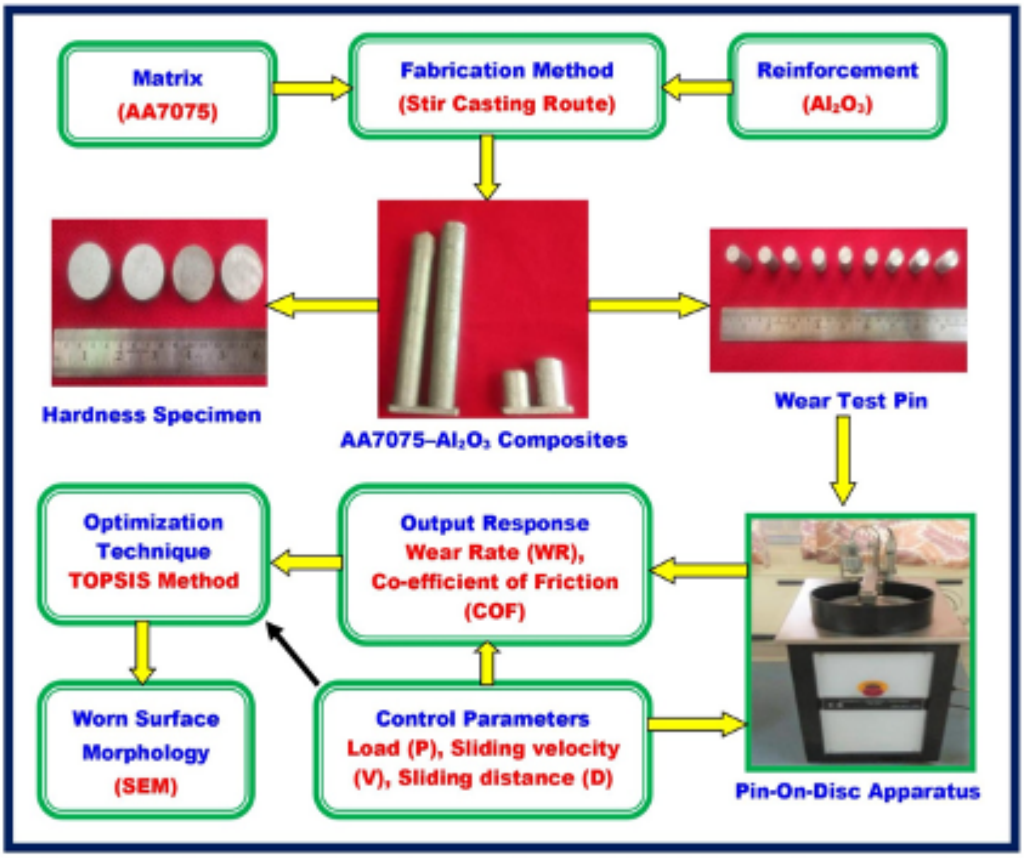

Figure 1. Experimental plan of present investigation.

Step1: Initially, the decision matrix D_{max} is formulated for the *m* alternatives and *n* attributes as follows,

$$D=\begin{bmatrix} X_{11} & X_{12} & \cdots & \cdots & X_{1j} \\ X_{21} & X_{22} & \cdots & \cdots & X_{2n} \\ \cdots & \cdots & \cdots & \cdots & \cdots \\ X_{i1} & X_{i2} & \cdots & X_{ij} & X_{in} \\ \cdots & \cdots & \cdots & \cdots & \cdots \\ X_{m1} & X_{m2} & \cdots & X_{mj} & X_{mn} \end{bmatrix}$$

where x_{ij} is the value of the optimal characteristics, where i = 1 − m is the number of results of each characteristic, and j = 1 − n is the number of characteristics to be optimized.

Step 2: The obtained values from decision matrix is normalized (r_{ij}) using Eq.(3):

$$r_{ij}=\frac{x_{ij}}{\sqrt{\sum_{i=1}^{m}x_{ij}^{2}}} \tag{3}$$

Table 1. L9 (3^3) array table with experimental results

Exp. No.	P (N)	V (m/s)	D (m)	WR (mm^3/m)	COF
1	10	1	500	0.005784	0.446
2	10	2	1000	0.004764	0.447
3	10	3	1500	0.004572	0.494
4	15	1	1000	0.002976	0.456
5	15	2	1500	0.005448	0.568
6	15	3	500	0.008016	0.543
7	20	1	1500	0.006084	0.602
8	20	2	500	0.008352	0.497
9	20	3	1000	0.006165	0.716

where i = 1, 2,…, m and j = 1, 2,…, n. x_{ij} represents the actual value of the i^{th} value of j^{th} experiment.

Step 3: The weighted normalized matrix is determined by the product of weight assigned for each response and the normalized value using Eq. (4)

$$v_{ij}=r_{ij}\times w_{j} \tag{4}$$

where w_j represents the weight of the j^{th} attribute w_j = 0.5, i = 1, 2,…, m and j = 1, 2,.., n. Table 2 illustrated the weighted normalized matrix.

Table 2. Normalized and weighted normalized matrix

Exp. No.	Normalized matrix		Weighted normalized matrix	
	WR	COF	WR	COF
1	0.333	0.346	0.166	0.173
2	0.345	0.396	0.172	0.198
3	0.348	0.377	0.174	0.189
4	0.374	0.333	0.187	0.167
5	0.337	0.371	0.168	0.185
6	0.312	0.300	0.156	0.150
7	0.330	0.243	0.165	0.121
8	0.310	0.295	0.155	0.147
9	0.306	0.311	0.153	0.156

Table 3. Separation measure and relative closeness

Exp. No.	Separation measure		Relative closeness C_i
	S_i^+	S_i^-	
1	0.078	0.110	0.585
2	0.050	0.130	0.724
3	0.047	0.126	0.729
4	0.003	0.170	0.982
5	0.078	0.093	0.542
6	0.143	0.055	0.276
7	0.099	0.072	0.422
8	0.150	0.068	0.312
9	0.122	0.061	0.332

Step 4: Positive ideal solution (A^+) and negative ideal solution (A^-) are calculated using Eq. (5) and Eq. (6)

$$A^+ = \left\{ \sum_{i=1}^{\max} v_{ij} \Big/ j \in J, \sum_{i=1}^{\min} v_{ij} \Big/ j \in J' \right\} \quad (5)$$

$$A^- = \left\{ \sum_{i=1}^{\min} v_{ij} \Big/ j \in J, \sum_{i=1}^{\max} v_{ij} \Big/ j \in J' \right\} \quad (6)$$

where, J is associated with the benefit parameters and J' - is associated with non-benefit parameters.

Step 5: The next step is to determine the separation measure for the positive ideal solution and negative ideal solution using Eq. (7) and Eq. (8):

$$S_i^+ = \sqrt{\sum_{j=1}^{n} \left(v_{ij} - A^+ \right)^2}, \text{ i=1, 2,…,m.} \quad (7)$$

$$S_i^- = \sqrt{\sum_{j=1}^{n} \left(v_{ij} - A^- \right)^2}, \text{ i=1, 2,…,m.} \quad (8)$$

Step 6: Finally, the relative closeness (C_i) of each alternative to the ideal solution is calculated using Eq. (9)

$$C_i = \frac{S_i^-}{S_i^+ + S_i^-} \quad (9)$$

The calculated separation measures and the relative closeness are provided in Table 3.

Step 7: Rank the relative closeness in ascending order. The higher rank will give the optimum combination of parameters. Figure 2 shows the rank plot for the obtained relative closeness (C_i). It reveals that the Ex. No 4 has a higher relative closeness (0.982), which consists of a better combination of optimal control parameter to obtain the lowest WR and COF.

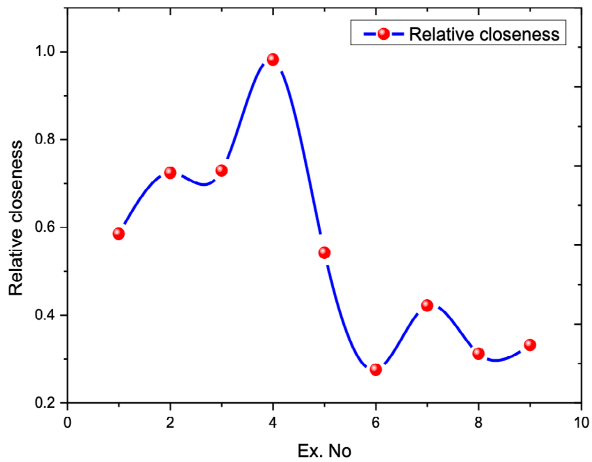

Figure 2. Rank plot for the relative closeness.

3. RESULTS AND DISCUSSION

3.1. Surface morphology

The surface morphology of the stir casted AA7075 matrix composites with varying compositions of Al_2O_3 particles were observed using a SEM. Figure 3(a-d) represents the SEM micrographs of unreinforced AA7075 and AA7075-Al_2O_3 composite specimens. From the Figs., the dark region represents the matrix alloy and white region represents the presence of the reinforcement (Al_2O_3 particles) content. In Fig. 3a, it can be ensure that there is no particles presence in the matrix. From Fig. 3(b-d), it was clearly reveal that a uniform dispersion of Al_2O_3 particles within the casted AA7075 matrix. It can also be clearly observed from the image that there was no formation of agglomerations or clusters of Al_2O_3 particles in the fabricated composites. This can be attributed to the utilization of appropriate stir casting parameters used to fabricate the

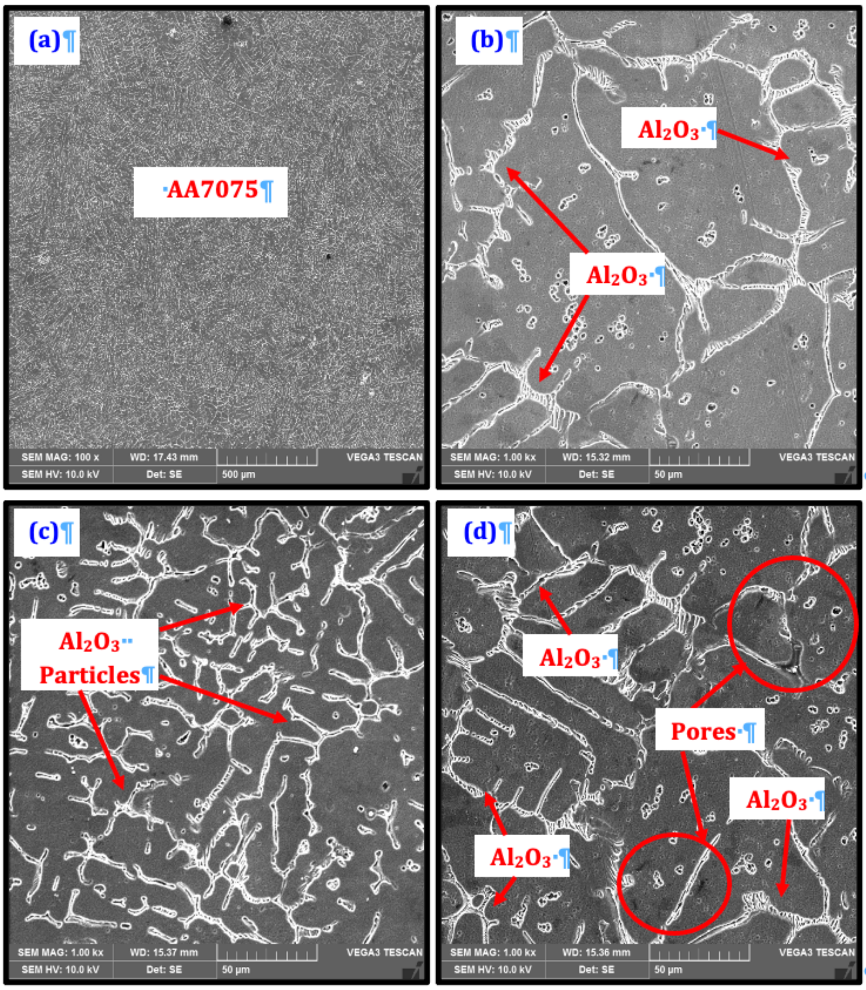

Figure 3. SEM micrograph (a) AA7075, (b) AA7075-4wt.% Al_2O_3, (c) AA7075-8wt.% Al_2O_3 and (d) AA7075-12wt.% Al_2O_3 composites.

composite specimen. However, the pores are formed in some regions in the AA7075-12 wt.% Al_2O_3 composite due to the gas entrapped in the molten metal.

3.2. Effect of Al_2O_3 particles on the hardness

Figure 4 represents the graphical data of the hardness measured at various locations in the composite samples. From Fig. 4, it can be noted that AA7075 – 8 wt.% Al_2O_3 composite shows better hardness and with minimum scatter in the measured points compared to the other three composites. With the addition of the hard reinforcement into the ductile matrix, the overall hardness of the composite is enhanced (Halverson *et al.,* 1989). It can be also observed that the presence of peaks and valleys are found in the values obtained for AA7075-12 wt.% Al_2O_3. The peak indicates that the reinforcing particles are agglomerated such that it gives maximum hardness and the valley in AA7075-12wt.% Al_2O_3 shows that absence of reinforcing particles at that location. This reveals that there exists inhomogeneities in the distribution of the reinforcing particles introduced in the AA7075-12wt.% Al_2O_3 and also indicates that the increase in content of the reinforcement above 8 wt.% leads to a poor distribution of the reinforcement particles in the matrix thus reducing the hardness (Sakthivelu *et al.,* 2019).

3.3. Effect of parameters on tribological behaviour

The main objective of this study was to determine the optimal levels of input parameters to obtain the lowest WR and COF under dry sliding condition. The mean of the relative closeness for each parameter levels are shown in Fig. 5. From the Fig, the x-axis represents the individual level of parameters such as load (P), sliding velocity (V) and sliding distance (D), and the y-axis represents the mean of relative closeness (C_i) value. In general, the optimum combination of parameters is identified by a higher relative closeness value. As it is seen in Fig. 5, it can be found that the optimum level of control parameters are the load at level 1 (P_1 = 10 N), the sliding velocity at lev-

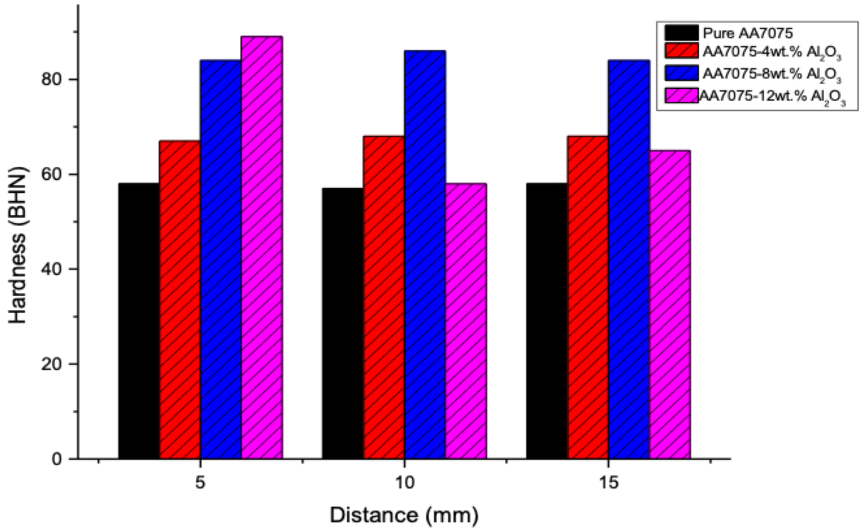

Figure 4. Brinell hardness of composites.

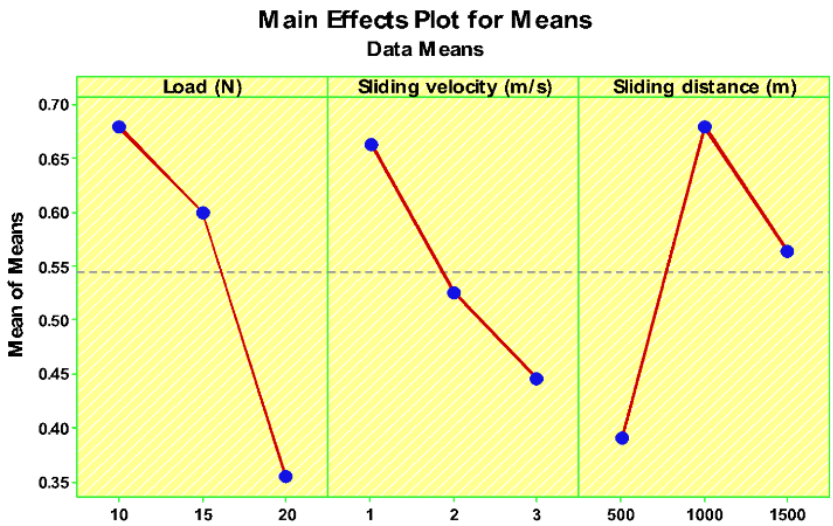

Figure 5. Main effect plot for relative closeness.

el 1 (V_1 = 1 m·s^{-1}) and the sliding distance at level 2 (D_2 = 1000 m), respectively. From the optimum condition we can observe that an increase in the load causes faster wear loss at the lowest sliding velocity and sliding distance. Normally, increasing the load and sliding distance causes higher wear loss because of the higher penetration of the abrasive particles into the specimen which ploughs the material from the specimen surface (Sahin, 2007). Here, the initial condition of load, sliding velocity and middle level of sliding distance provide the lowest WR and COF for the fabricated AA7075-Al_2O_3 composites.

Table 4 depicts the response table for the mean relative closeness (C_i) with respect to each level of control parameters. From the table, it has been revealed the influence of the control parameters for

Table 4. Means table for relative closeness

Level	P (N)	V (m/s)	D (m)	Average mean relative closeness (C_i)
1	0.6793	0.6632	0.3912	
2	0.6000	0.5259	0.6794	
3	0.3554	0.4457	0.5643	0.5448
Delta	0.3239	0.2175	0.2882	
Rank	1	3	2	

the lowest WR and COF. As it is seen in Table 4, it can be observed that the load (P) takes rank 1 which plays a dominant role in obtaining the lowest WR and COF, followed by the sliding distance (D) and the sliding velocity (V) respectively. By employing the ANOVA analysis, this observation was ensured. ANOVA is a statistical tool which is widly used to determine the influence of parameters on the response (Agarwal *et al.,* 2023). Hence, in this study, an ANOVA was performed to find out the impact of control parameters namely 'P', 'V' and 'D' on the WR and COF of the AA7075-8 wt.% Al_2O_3 composite using a dry sliding wear test. The results were reported in Table 5 and also the graphical representation of parameters contribution is shown in Fig. 6. Based on the results in Fig. 6, it can be concluded that the load is the primary dominant factor with a contribution of P = 38.36%, followed by the sliding distance, D = 28.32% and the sliding velocity, V = 16.27% respectively. The similar results were previously observed by Dhanalakshmi *et al.* (2018) after performing dry sliding wear tests on Al7075-Al_2O_3-B_4C composites and they reported that the load was the primary impact factor affecting the tribological behaviour.

Table 5. ANOVA for relative closeness

Source	DF	Seq SS	Adj SS	Adj MS	F-value
P	2	0.171	0.171	0.086	2.270
V	2	0.073	0.073	0.036	0.960
D	2	0.126	0.126	0.063	1.670
Error	2	0.076	0.076	0.038	--
Total	8	0.445	--	--	--

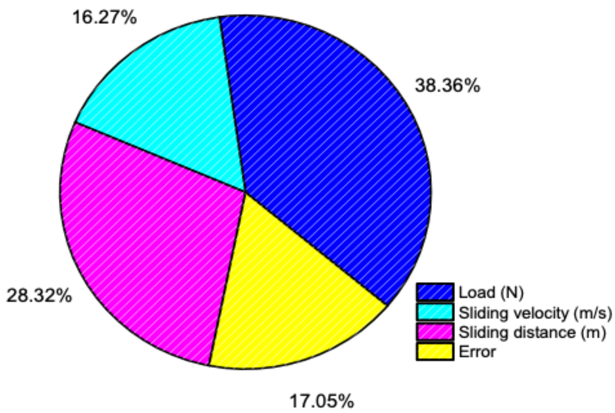

Figure 6. Contribution plot of the different parameters.

Figure 7 (a-c) shows the contour mapping of the WR for the tested AA7075 matrix composites reinforced with Al_2O_3 particles with respect to the control parameters, namely, load (P), sliding velocity (V) and sliding distance (D), respectively. The interaction effect of load versus sliding velocity on the WR is presented in Fig. 7a. As the load and sliding velocity increased simultaneously, there was an improvement in the WR. However, the lowest WR (0.0003 mm^3/m) is achieved at the moderate load and initial sliding velocity conditions. Meanwhile, the maximum load of 20 N with medium sliding velocity of 2 $m \cdot s^{-1}$ gave the highest WR (>0.008 mm^3/m). Fig. 7b reveals the effect of load versus sliding distance on the WR of the tested composite. It was clearly observed that the lowest WR is attained for 1000 m of sliding distance and a load of 15 N. But, with an increase in the load at the initial sliding distance of 1000 m produce more WR. This is because the maximum load creates a high pressure on the composite pin thus leading to an increase in the WR. Fig. 7c

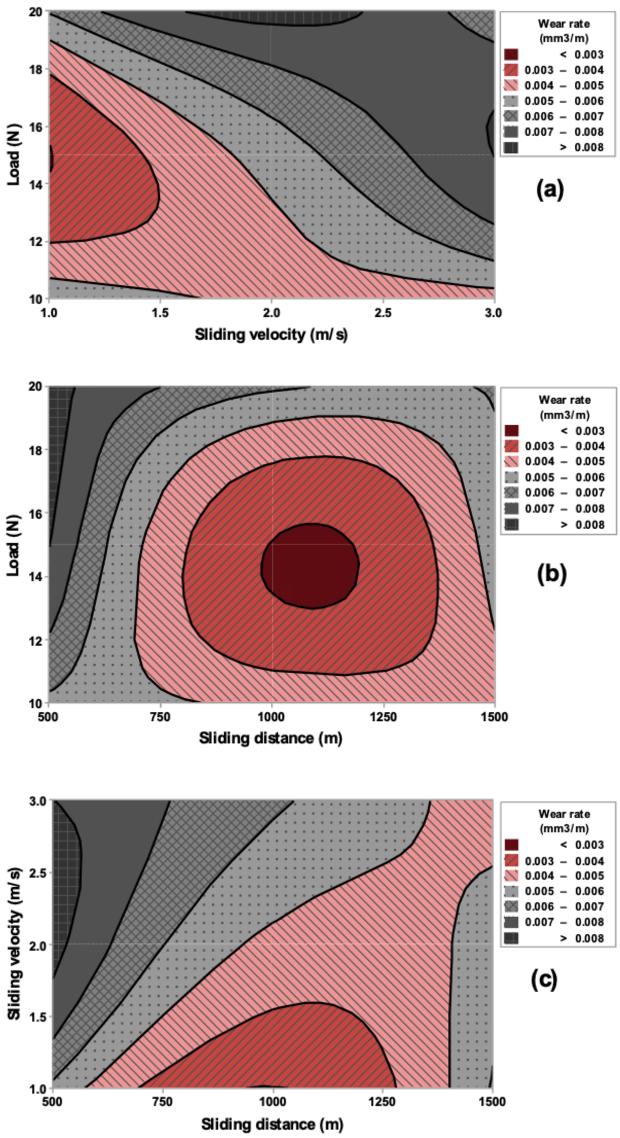

Figure 7. Contour plot of WR (a) P vs. V, (b) P vs. D and (c) V vs. D.

represents the effect of the sliding velocity and sliding distance on the WR. It can be understood that a lower sliding velocity (1 $m \cdot s^{-1}$) with moderate sliding distance (1000 m) produces a low WR. Similarly, the maximum WR was obtained for the lowest sliding distance (500 m) using the highest sliding velocity (3 $m \cdot s^{-1}$).

The contour mapping of the COF for the AA7075-8 wt.% Al_2O_3 composites with respect to the wear control parameters. Namely, load (P), sliding velocity (V) and sliding distance (D) are illustrated in Fig. 8(a-c). The interactive effect of load versus sliding distance on the COF of the tested composite is depicted in Fig. 8a. It was found that the lowest COF (<0.45) is obtained at the lowest applied load of 10 N and sliding velocity of 1 $m \cdot s^{-1}$

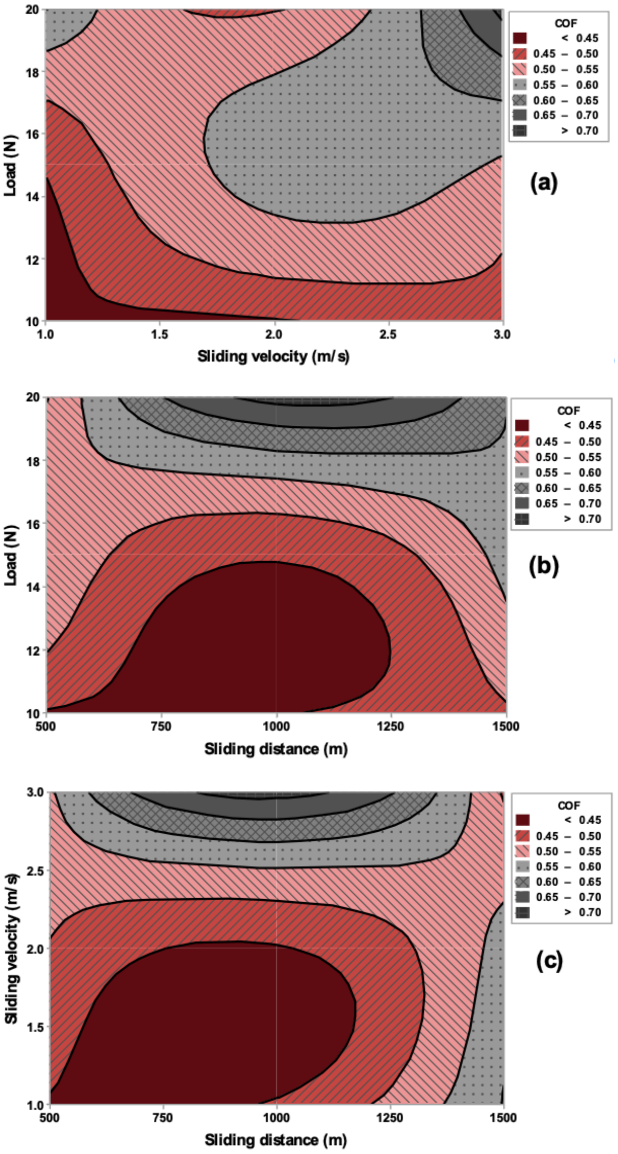

Figure 8. Contour plot of COF (a) P vs. V, (b) P vs. D and (c) V vs. D.

respectively. At the same time, the COF gradually increased with an increase in the load and sliding velocity. However, the load of 10 N using 3 $m \cdot s^{-1}$ as the sliding velocity produced greater COF (>0.70). Fig. 8b demonstrates the influence of the sliding velocity versus the sliding distance on the COF. It has been noticed that the lowest COF (<0.45) was obtained for the middle level of sliding distance (1000 m) using a load from 10 N to 15 N. Furthermore, the COF is increased with an increase in the load to a maximum level of 20 N and using sliding distance of 1000 m respectively. Figure 8c shows the effect of the sliding distance and the sliding velocity on the COF of the casted composite during the dry sliding wear tests. It clearly reveals that the lowest COF is obtained for the medium level of the sliding distance (1000 m) and using 2 $m \cdot s^{-1}$ as sliding velocity. However, an increase in the sliding velocity produces more COF at the middle level of sliding distance.

3.4. Confirmation experiments

The final step in the tribological behaviour analysis of AA7075-8 wt.% Al_2O_3 composite was to validate the predicted result and, for this purpose, a confirmation experiment was conducted by considering the optimized parameters' conditions as shown in Table 6. It was revealed that the relative closeness (C_i) values for the experimental and predicted control parameters are 0.982 and 0.9323 respectively. Based on the results, a very low percentage error of 5.06% was obtained between the experimental and predicted results which ensures the very good correlation.

Table 6. Confirmation experiments

Parameter setting	Optimal level	Wear rate (mm^3/m)	COF	Relative closeness (C_i)	Error (%)
Experimental	$P_2V_1D_1$	0.002976	0.456	0.982	5.06
Predicted	$P_1V_1D_2$	-	-	0.9323	

3.5. Worn surface morphology

Figure 9a represents the worn surface morphology of the AA7075-Al_2O_3 composite for the initial parametric conditions. From this figure, we can observe the deep ploughs present in the surface. This is due to the impregnation of the counter disc particles at the loading conditions. This leads to the ploughing of a large volume of particles from the base AA7075 which results in a higher wear rate. Figure 9 (b-c) shows the worn out surface morphology for the confirmation experiment sample AA7075-8 wt.% Al_2O_3 to understand the abrasive wear mechanism. Figure

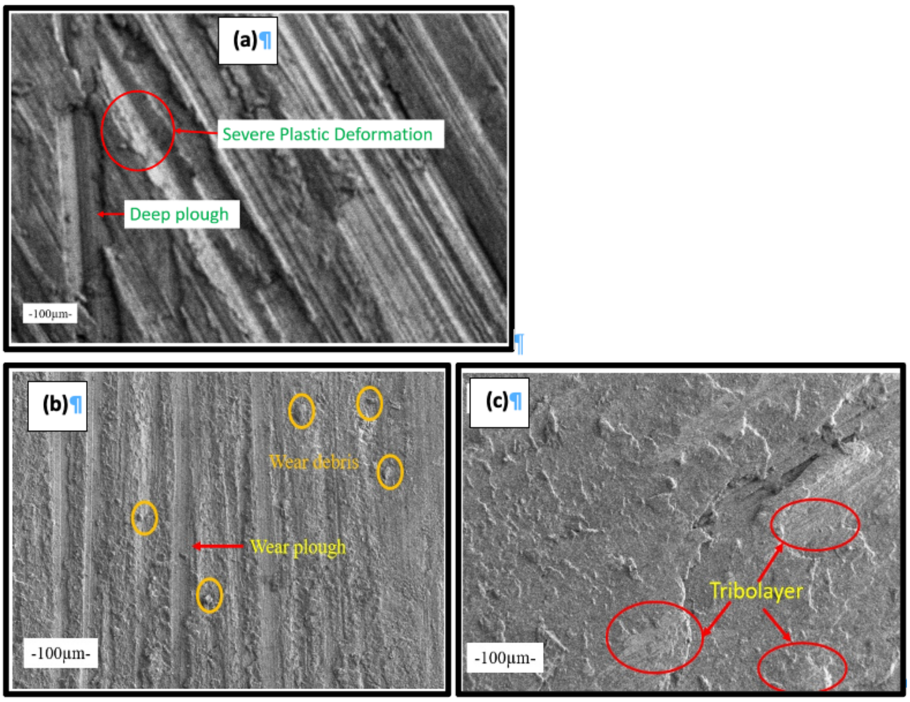

Figure 9. SEM image of AA7075-8 wt.% Al_2O_3 worn surface (a) for initial condition, and (b, c) for optimal combination of parameters.

9b reveals the impregnation of abrasive particles into the sample, forming a deeper plough. The increase in the load leads to the formation of plough. It can be understood that the increase in the load increases the wear loss; besides the contact between the abrasive particles and specimen also increases which leads to an increase in the COF. As the sliding velocity increases, the formation of wear debris will be reduced due to the low interaction between the abrasive particles and the specimen surface. This phenomenon shows that the wear rate will decrease by increasing the sliding velocity (Dharmalingam *et al.,* 2013). It can also be concluded that the worn surface for the highest load has a significant delamination, which was likely brought on by the development of a high temperature at the interfaces. This delamination is due to the high amount of metal deformation and increased material removal caused by the frictional heat buildup between the two surfaces which are in intense contact. Thus, while combining severe delamination with an increasing load, moderate adhesion wear was achieved. Figure 9c represents the formation of a tribo-layer due to the increase in temperature between the abrasive wheel and the composite pin. Because of the formation of a tribo-layer, the friction coefficient is minimized, which improves the wear resistance of the composites (Balaji *et al.,* 2022). In addition to that, the incorporation of Al_2O_3 particles is the main reason for the enhancement of the wear resistance because of the high hardness of the composite compared to the base alloy.

CONCLUSIONS

- AA7075 matrix composites with varying amounts of Al_2O_3 particles (4, 8 and 12 wt.%) were synthesized successfully through the stir casting technique.
- The surface morphology of the prepared composite ensured that the Al_2O_3 particles are uniformly dispersed within the matrix. The hardness of the synthesized specimens was measured at different locations, finding that the maximum hardess was obtained for the AA7075 – 8 wt.% Al_2O_3 composite.
- Based on the hardness value, AA7075 – 8 wt.% Al_2O_3 composite was utilized to predict the tribological behavior under dry conditions and the control parameters were optimized using TOPSIS approach.
- TOPSIS method stated that optimal conditions of control parameters were found to be L= 10 N, V= 1 $m \cdot s^{-1}$ and D= 1000 m. The predicted results obtained were validated conducting a confirmation experiment, obtaining a low error (-5.4%).
- ANOVA was carried out to understand the individual contribution of process parameters for the lowest WR and COF. ANOVA result reveals that the load was the primary decisive factor with a contribution of 38.36%, trailed by sliding distance (28.32%) and sliding velocity (16.27%) respectively.

- The wear mechanism was studied inspecting the worn surface by scanning electron microscopy. It was observed that the wear loss is minimized due to the inclusion of Al_2O_3 particles.
- In the future, the dry sliding wear parameters for the produced composites will be investigated using other optimization techniques like artificial neural networks and genetic algorithms.

REFERENCES

Agarwal, V., Goyal, D., Pabla, B.S., Vettivel, S.C., Haiter Lenin, A. (2023). Optimization and characterization studies of dissimilar friction stir welding parameters of brass and aluminum alloy 6063 using Taguchi method. *Adv. Mater. Sci. Eng.* 1-10. ID 8275323. https://doi.org/10.1155/2023/8275323.

Akinwamide, S.O., Lemika, S.M., Obadele, B.A., Akinribide, O.J., T. Abe, B., Olubambi, P.A. (2019). Characterization and mechanical response of novel Al-(Mg–TiFe–SiC) metal matrix composites developed by stir casting technique. *J. Compos. Mater.* 53, 3929-3938. https://doi.org/10.1177/002199831985119.

Alagarsamy, S.V., Ravichandran, M. (2019a). Synthesis, microstructure and properties of TiO_2 reinforced AA7075 matrix composites via stir casting route. *Mater. Res. Express.* 6, 1-15. https://doi.org/10.1088/2053-1591/ab1d3b.

Alagarsamy, S.V., Ravichandran, M. (2019b). Investigations on tribological behaviour of AA7075-TiO_2 composites under dry sliding conditions. *Ind. Lubr. Tribol.* 71 (9), 1064-1071. https://doi.org/10.1108/ILT-01-2019-0003.

Alagarsamy, S.V., Raveendran, P., Ravichandran, M. (2020). Investigation of material removal rate and tool wear rate in spark erosion machining of Al-Fe-Si alloy composite using Taguchi coupled TOPSIS approach. *Silicon.* 13, 2529-2543. https://doi.org/10.1007/s12633-020-00596-x.

Altinkok, N. (2013). Mechanical properties and wear behaviour of Al_2O_3/SiC_p reinforced aluminium-based MMCs produced by the stir casting technique. *Adv. Compos. Lett.* 22 (4), 80-89. https://doi.org/10.1177/096369351302200402.

Allasi, H.L., Soosaimariyan, M.V., Chidambaranathan, V.S. (2023). Wear behaviour of a Cu-Ni-Sn hybrid composite reinforced with B4C prepared by powder metallurgy technique. *J. Mech. Eng.* 69 (5-6), 275–283. https://doi.org/10.5545/sv-jme.2022.423.

Azadeh, A., Kor, H., Hatefi, S.-M. (2011). A hybrid genetic algorithm-TOPSIS-computer simulation approach for optimum operator assignment in cellular manufacturing systems. *J. Chin. Inst. Eng.* 34 (1), 57-74. https://doi.org/10.1080/02533839.2011.552966.

Balaji, S., Maniarasan, P., Alagarsamy, S. V., Alswieleh, A.M., Mohanavel, V., Ravichandran, M., Jeon, B.H., Allasi, H.L. (2022). Optimization and prediction of tribological behaviour of Al-Fe-Si alloy based nano grains refined composites using Taguchi with response surface methodology. *J. Nanomater.* 1-12, ID 9733264. https://doi.org/10.1155/2022/9733264.

Baskaran, S., Anandakrishnan, V., Duraiselvam, M. (2014). Investigations on dry sliding wear behavior of in situ casted AA7075–TiC metal matrix composites by using Taguchi technique. *Mater. Des.* 60, 184-192. https://doi.org/10.1016/j.matdes.2014.03.074.

Bharath, V., Nagaral., M., Auradi, V., Kori, S.A. (2014). Preparation of 6061Al-Al_2O_3 MMC's by stir casting and evaluation of mechanical and wear properties. *Procedia. Mater. Sci.* 6, 1658 – 1667. https://doi.org/10.1016/j.mspro.2014.07.151.

Bhowmik, A., Dey, D., Biswas, A. (2021). Comparative study of microstructure, physical and mechanical characterization of SiC/TiB_2 reinforced aluminium matrix composite. *Silicon.* 13, 2003–2010. https://doi.org/10.1007/s12633-020-00591-2

Dhanalakshmi, S., Mohanasundararaju, N., Venkatakrishnan, P.G., Karthik, V. (2018). Optimization of friction and wear behaviour of Al7075-Al_2O_3-B_4C metal matrix composites using Taguchi method. *IOP Conf. Series: Mater. Sci. Eng.* 314, 012025. https://doi.org/10.1088/1757-899X/314/1/012025.

Dharmalingam, S., Subramanian, R., Kok, M. (2013). Optimization of abrasive wear performance in aluminium hybrid metal matrix composites using Taguchi–grey relational analysis. *Proc. Inst. Mech. Eng. J: J. Eng. Tribol.* 227 (7), 749-760. https://doi.org/10.1177/13506501124679.

Halverson, D.C., Pyzik, A.J., Aksay, I.A., Snowden, E. (1989). A processing of boron carbid –aluminium composites. *J. Am. Ceram. Soc.* 72 (5), 775–780. https://doi.org/10.1111/j.1151-2916.1989.tb06216.x.

Huda, A. Al-Salihi, Akram Mahmood, A., Hussain J. Alalkawi. (2019). Mechanical and wear behavior of AA7075 aluminum matrix composites reinforced by Al_2O_3 Nanoparticles. *Nanocomposites.* 5 (3), 67-73. https://doi.org/10.1080/20550324.2019.1637576.

Jayakumar, E., Praveen, A.P., Rajan, T.P.D., Pai, B.C. (2018). Studies on tribological characteristics of centrifugally cast SiC_p-reinforced functionally graded A319 aluminium matrix composites. *Trans. Indian. Inst. Met.* 71, 2741–2748. https://doi.org/10.1007/s12666-018-1442-5.

Johny James, Jabanjalin, H., Ahaiter L. (2023). Study of tribological and mechanical properties of composite reinforced with tungsten carbide. *AIP Conf. Proc.* 2548 (1), 050007. https://doi.org/10.1063/5.0121012.

Magibalan, S., Senthilkumar, P., Senthilkumar, C., Prabu, M. (2020). Optimization of wear parameters for aluminium 4% fly-ash composites. *Indian J. Eng. Mater. Sci.* 27, 458-464.

Mistry, J.M., Gohil, P.P. (2019). Experimental investigations on wear and friction behaviour of Si3N4p reinforced heat-treated aluminium matrix composites produced using electromagnetic stir casting process. *Compos. Part B: Eng.* 161, 190-204. https://doi.org/10.1016/j.compositesb.2018.10.074.

Miyajima, T., Iwai, Y. (2003). Effects of reinforcements on sliding wear behaviour of aluminium matrix composites. *Wear* 255 (1-66), 606-616. https://doi.org/10.1016/S0043-1648(03)00066-8.

Moustafa, E.B., Mikhaylovskaya, A.V., Taha, M.A., Mosleh, A.O. (2022). Improvement of the microstructure and mechanical properties by hybridizing the surface of AA7075 by hexagonal boron nitride with carbide particles using the FSP process. *J. Mater. Res. Technol.* 17, 1986-1999. https://doi.org/10.1016/j.jmrt.2022.01.150.

Sahin, Y. (2007). Tribological behaviour of metal matrix and its composite. *Mater. Des.* 28, 1348-1352. https://doi.org/10.1016/j.matdes.2006.01.032.

Sakthivelu, S., Sethusundaram, P.P., Meignanamoorthy, M., Ravichandran, M. (2018). Synthesis of metal matrix composites through stir casting process-a review. *Mech. Mech. Eng.* 22 (1), 357-370.

Sakthivelu, S., Meignanamoorthy, M., Ravichandran, M., Sethusundaram, P.P. (2019). Tribological behaviour of AA7075-$ZrSiO_4$ composites synthesized by stir casting technique. *Mech. Mech. Eng.* 23, 198-201. https://doi.org/10.2478/mme-2019-0026.

Sambathkumar, M., Sasikumar, K.S.K., Gukendran, R., Dineshkumar, K., Ponappa, K., Harichandran, S. (2021). Investigation of mechanical and corrosion properties of Al7075/Redmud metal matrix composite. *Rev. Metal.* 57 (1), e185. https://doi.org/10.3989/revmetalm.185.

Senthamarai, K., Deepak, D., Saravanan, H., Gopikrishnan, C., Alagarsamy, S.V., Chanakyan, C. (2023). Investigations on the wire EDM characteristics of Al matrix composite using TOPSIS method. *Mater. Today: Proc.* 74 (1), 110-116. https://doi.org/10.1016/j.matpr.2022.12.130.

Singh, J., Chauhan, A. (2019). A review of microstructure, mechanical properties and wear behavior of hybrid aluminium matrix composites fabricated via stir casting route. *Sadhana* 44, 16. https://doi.org/10.1007/s12046-018-1025-5.

Suresh, S., Gowd, G.H., Deva Kumar, M.L.S. (2019). Mechanical properties of AA 7075/Al_2O_3/SiC nano-metal matrix composites by stir-casting method. *J. Inst. Eng. India Ser. D.* 100, 43–53. https://doi.org/10.1007/s40033-019-00178-1.

Uros Stamenkovic., Svetlana Ivanov., Markovic., I., Milan Gorgievski, Božinović, K., Kovačević, A. (2023). The influence of the ageing temperature on different properties of the EN AW-7075 aluminium alloy. *Rev. Metal.* 59 (1), e238. https://doi.org/10.3989/revmetalm.238.